High-efficiency ozone generation using a multi-chamber coaxial dielectric barrier discharge system for water treatment

Brian Risnugroho[1], *Moch* Dhofir[1], *Corina* Martineac[2], *Tri* Nurwati[1], *Hadi* Suyono[1], and *Rini Nur* Hasanah[1*]

[1]Electrical Engineering Department, Universitas Brawijaya, Malang 65145, Indonesia
[2]Electrical Engineering Faculty, Technical University of Cluj-Napoca, 400114 Romania

Abstract. This paper presents the design, modeling, and experimental evaluation of a multi-chamber coaxial Dielectric Barrier Discharge (DBD) reactor for enhanced ozone generation in water-treatment applications. The proposed reactor employs axially staged discharge chambers to increase effective ionization volume without increasing local electric-field stress. Finite-element simulations confirm strong electric-field localization within the 1-mm air gap, achieving peak intensities up to 145 kV/cm at 15 kV while preserving dielectric integrity. Experiments were conducted at applied voltages of 5–15 kV, airflow velocities of 2 m/s and 5 m/s, and treatment durations up to 10 minutes. Ozonation performance was evaluated using CIE Lab* colorimetric analysis. Results show that higher applied voltage significantly enhances chromatic degradation due to intensified ionization activity. Lower airflow velocity (2 m/s) improves ozone utilization by extending residence time, while increasing the chamber count from one to three chambers enables cumulative plasma exposure and near-complete decolorization under optimal conditions (15 kV, 2 m/s). Power analysis reveals increased electrical consumption with additional chambers, indicating a performance–energy trade-off. Energy-normalized evaluation demonstrates that although total decolorization increases, efficiency per unit power decreases slightly. The estimated ozone production rate for the three-chamber configuration at 15 kV ranges from 0.8 to 4.8 g/h. The proposed staged architecture provides a scalable strategy for balancing ozone output and energy efficiency.

1 Introduction

Ozone (O_3) is widely used in sterilization, oxidation, and advanced water-treatment applications due to its strong oxidative capability and environmentally benign characteristics. Conventional ozone-generation techniques, such as corona discharge and ultraviolet (UV) irradiation, suffer from limitations in energy efficiency and operational stability. In contrast, Dielectric Barrier Discharge (DBD) systems have emerged as a promising alternative, as they are capable of generating non-thermal plasma with high electron energy while maintaining low gas temperatures.

Recent studies have reported significant improvements in ozone generation through optimized DBD geometries, including planar and tubular reactors [1], hybrid DBD configurations [2], and coaxial DBD systems employing perforated electrodes [3]. Despite these advances, investigations focusing on multi-chamber coaxial DBD architectures, which potentially provide increased ionization volume and improved electric-field uniformity, remain limited.

To address this research gap, this paper presents the development of a compact coaxial DBD reactor with a configurable chamber count ranging from one to three chambers. The proposed design aims to enhance electric-field intensity and ozone-production efficiency through staged plasma generation along the airflow direction. This study integrates: (1) electric-field analysis using analytical formulations and finite-element-method (FEM) simulations, (2) experimental evaluation of ozone-generation effectiveness using a colored-water degradation test quantified by CIE Lab* colorimetry, and (3) assessment of energy efficiency through leakage-current and power-loss measurements. The proposed system is intended for environmentally compatible water-treatment applications and builds upon recent developments in ozone-based advanced oxidation processes (AOPs) [4]-[6].

Unlike previously reported coaxial DBD systems that primarily focus on single-discharge regions or electrode-shape optimization, the present work introduces a staged axial multi-chamber architecture that enables cumulative plasma exposure along the airflow direction without increasing local electric-field stress. This approach enhances the effective ionization volume while preserving dielectric integrity and operational stability. The proposed modular configuration provides a scalable design strategy for improving ozone generation performance through geometric extension rather than excessive voltage escalation.

Accurate characterization of discharge power and ozone yield remains a critical aspect of DBD reactor

* Corresponding author: rini.hasanah@ub.ac.id

optimization, as emphasized in comprehensive studies on DBD plasma physics and diagnostics [7], [8].

Unlike conventional single-discharge coaxial DBD systems, the present work introduces an axially staged multi-chamber configuration that enhances cumulative plasma exposure while maintaining constant electric-field stress across the dielectric barrier.

2 Materials and methods

2.1 Reactor design

The high-electric-field generation system employed for ozone production in this study is illustrated in Figure 1. The proposed ozone reactor utilizes a coaxial electrode configuration, as shown in Figure 2. The system consists of a stainless-steel rod inner electrode with a radius of 3 mm ($r0$), an annular air gap of 1 mm serving as the discharge region, and a dielectric layer formed by an acrylic tube with an inner radius of 4 mm ($r1$) and an outer radius of 5 mm ($r2$). A cylindrical grounded outer electrode encloses the dielectric layer.

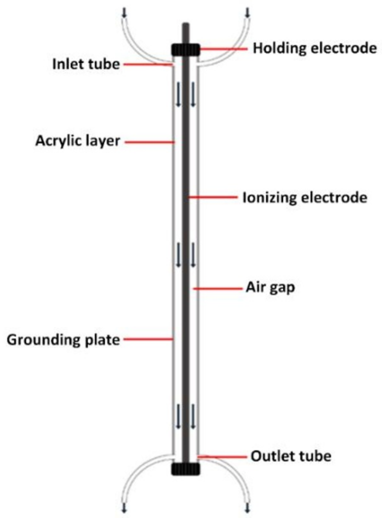

Fig. 1. Design of coaxial high electric field generation system for ozone reactor.

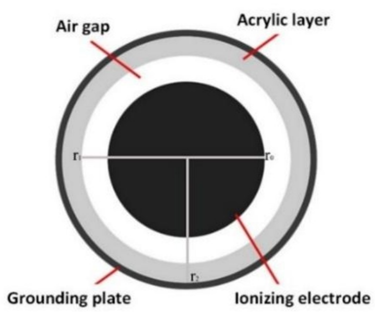

Fig. 2. Structure of multilayer dielectric coaxial electrodes.

This configuration was designed to concentrate a high electric field within the air gap, which is the primary region for ionization and ozone formation. Reactor configurations with one, two, and three chambers were fabricated by axially aligning multiple coaxial dielectric–electrode units along the airflow direction. Air was supplied axially through the reactor at flow velocities of 2 m/s and 5 m/s.

2.2 Materials

The materials used in the experimental setup include a colored aqueous solution as an indicator of the ozone-based purification process, a high-voltage test transformer (220 V/100 kV, 5 kVA, 50 Hz), a 100-pF measurement capacitor (CM) functioning as a voltage divider prior to the digital storage multimeter (DSM), and an AC voltage measurement device (DSM). Electrical connections between the transformer secondary and the inner electrode were established using NYA conductor cables (2 mm diameter). An air compressor was used to supply airflow through pipes and hoses into the ozone reactor, while an aerator stone was employed to disperse air bubbles uniformly. An anemometer was utilized to measure airflow velocity. Additional components included stainless-steel rod electrodes, multilayer coaxial dielectric structures, and mechanical baffles for electrode fixation.

2.3 Electric-field modeling and simulation

The electric-field distribution within the multilayer coaxial dielectric structure was analyzed using analytical formulations derived for coaxial geometries and validated through finite-element-method (FEM) simulations. The radial electric-field intensity in each dielectric layer is given by

$$E_i(r) = \frac{U}{r\varepsilon_i \sum_{j=1}^{n} \frac{1}{\varepsilon_j} \ln\left(\frac{r_j}{r_j-1}\right)} \quad , \quad r_i - 1 < r < r_i \qquad (1)$$

where U is the applied voltage, εi is the permittivity of the i-th dielectric layer, and indices i and j denote the respective layer numbers in the multilayer coaxial structure. The relative permittivity values used in this study were εr=1 for air and εr=4 for acrylic.

Simulations were performed for applied voltages of 5 kV, 10 kV, and 15 kV to determine peak electric-field intensities and spatial field distributions across the air and dielectric layers.

2.4 Experimental set-up

The experimental circuit used to evaluate ozone-generation effectiveness is shown in Figure 3, while the circuit employed for energy-efficiency analysis through leakage-current measurement is presented in Figure 4.

In the ozone-generation experiment, high-voltage AC input ranging from 5 kV to 15 kV was applied to the inner electrode. Airflow was regulated using an anemometer-calibrated blower, and colored-water samples were employed as visual indicators of ozone-induced degradation.

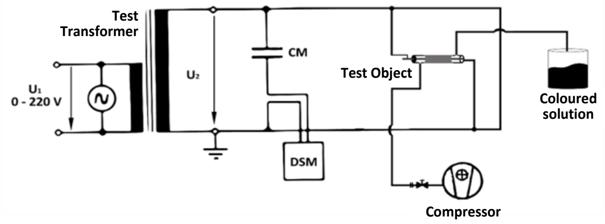

Fig. 3. Experimental circuit for evaluating ozonation effectiveness.

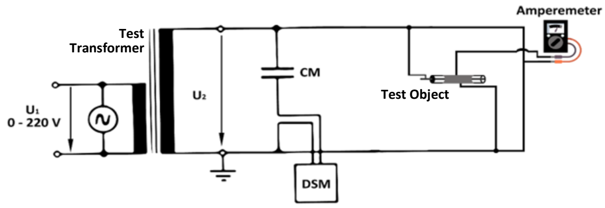

Fig. 4. Experimental circuit for leakage-current measurement.

Using the setup shown in Figure 4, the discharge-related apparent power was estimated from the measured leakage current and the applied high-voltage AC (HV-AC) voltage during the discharge process.

2.5 Evaluation metrics

2.5.1 Ozonation effectiveness

Ozonation effectiveness was quantified using the CIE Lab* color space (CIELAB), with particular emphasis on the a* parameter. A decrease in positive a*-values indicates successful degradation of red chromatic components in the solution. In this study, ozonation effectiveness was classified based on the final a* value, where $0 < a^* \leq 2$ represents high decolorization, $a^* \leq 0$ indicates very high (complete) decolorization, and $2 < a^* \leq 5$ corresponds to moderate effectiveness.

2.5.2 Energy Efficiency

Energy efficiency was evaluated by estimating the electrical power associated with the discharge process using

$$P_{loss} = U.I \tag{2}$$

where U is the applied voltage and I is the measured leakage current during the discharge process. It is well established that accurate discharge power determination in dielectric barrier discharge (DBD) systems is ideally performed using charge–voltage (Q–V) Lissajous analysis or synchronized voltage–current waveform measurements to evaluate real plasma power per cycle [7], [8]. These methods integrate the energy enclosed by the Lissajous figure and provide a more rigorous representation of discharge power compared to apparent power estimation.

In the present study, phase-angle measurements were not implemented; therefore, the reported values represent apparent discharge power primarily for comparative analysis among configurations.

3 Results and discussion

3.1 Electric-field distribution and discharge characteristics

Finite-element-method (FEM) simulations were performed to characterize the electric-field distribution within the multilayer coaxial structure under applied voltages of 5 kV, 10 kV, and 15 kV. The simulated electric-field spectrum is shown in Figure 5, while the radial field distribution at 10 kV is presented in Figure 6.

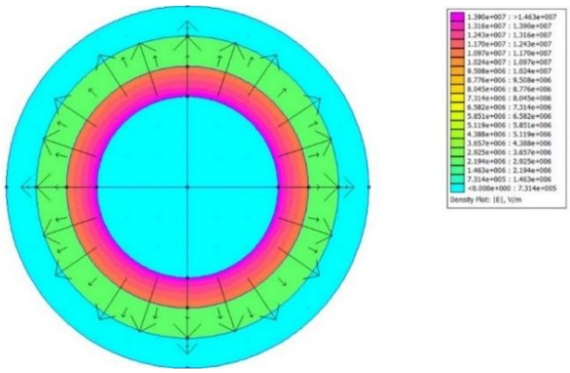

Fig. 5. Simulated electric-field intensity distribution in the multilayer coaxial DBD reactor obtained using finite-element-method (FEM) simulation.

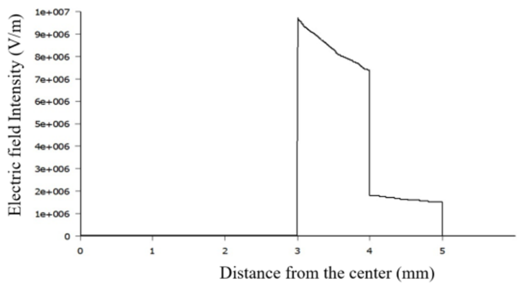

Fig. 6. Radial electric-field intensity distribution within the multilayer coaxial structure at 10 kV applied voltage.

As expected for coaxial geometries, the electric field is strongly concentrated within the 1-mm annular air gap, particularly near the high-voltage inner electrode. Peak electric-field intensities of approximately 48 kV/cm, 97 kV/cm, and 145 kV/cm were obtained for applied voltages of 5 kV, 10 kV, and 15 kV, respectively. In contrast, the electric-field magnitude decreases significantly within the acrylic dielectric layer due to its higher relative permittivity ($\varepsilon r = 4$), ensuring dielectric protection and operational safety.

The radial decay of the electric field follows the theoretical behavior predicted for multilayer coaxial dielectric systems, confirming the validity of the analytical formulation introduced in Section 2.3. These results indicate that increasing the applied voltage directly enhances ionization intensity within the discharge region without imposing excessive electric stress on the dielectric barrier. This controlled field localization forms the physical basis for improved ozone generation observed in subsequent experiments.

The observed field localization within the air gap is consistent with established DBD discharge behavior, where electron acceleration and microdischarge formation are governed by strong local electric-field gradients in dielectric-barrier configurations [7], [8].

3.2 Influence of applied voltage and treatment duration

The influence of applied voltage on ozonation effectiveness was evaluated using CIE Lab* colorimetric analysis, with the a* parameter serving as the primary indicator of chromatic degradation. As summarized in Table 1, increasing the applied voltage from 5 kV to 15 kV significantly reduces the a* value after 1 minute of treatment.

Table 1. Observation of the effect of applied voltage on the change in solution clarity (1 chamber, 2 m/s, 1 minute).

Applied Voltage		5 kV	10 kV	15 kV
Solution Color				
HEX		B01251E	AD3330	925F42
RGB	RED	176	173	146
	GREEN	37	51	95
	BLUE	30	48	66
CIE Lab*	L	38.98	40.35	45.20
	a	54.35	49.20	17.51
	b	39.57	30.62	25.04

At 15 kV, the substantial reduction in a* indicates enhanced ozone formation resulting from stronger electron acceleration and increased ionization events within the air gap. This observation is consistent with previously reported quasi-linear relationships between applied voltage and ozone generation rate in atmospheric-pressure DBD systems [2].

Treatment duration also plays an important role, particularly at lower voltages. As shown in Table 2, progressive reduction of the a* value occurs with increasing exposure time. However, at 5 kV, extended treatment duration is required to achieve substantial decolorization, indicating that electric-field strength remains the dominant factor governing ozone production efficiency.

Table 2. Observation of the effect of airflow injection time duration on the change in solution clarity (1 chamber, 5 kV, 2 m/s).

Time duration		1 min	3 mins	5 mins	10 mins
Solution Color					
HEX		B0251E	AD3E33	966441	897246
RGB	RED	176	173	150	137
	GREEN	37	62	100	114
	BLUE	30	51	65	70
CIE Lab*	L	38.98	42.11	46.95	49.25
	a	54.35	44.71	16.28	2.88
	b	39.57	30.89	27.91	27.66

These findings collectively demonstrate that voltage escalation enhances instantaneous ozone formation, while exposure duration controls cumulative oxidation effects.

3.3 Effect of airflow rate on ozone utilization

Airflow velocity influences both plasma stability and ozone residence time within the reactor. Table 3 compares ozonation performance at airflow rates of 2 m/s and 5 m/s under identical voltage conditions.

Operation at 2 m/s consistently produces greater chromatic degradation than at 5 m/s. Although higher airflow improves gas refreshment in the discharge region, it simultaneously reduces ozone residence time and limits ozone–liquid mass transfer efficiency. In contrast, lower airflow velocity increases contact duration and promotes more stable plasma formation, thereby improving effective ozone utilization.

Table 3. Observation of the effect of airflow rate on the change in solution clarity (1 chamber, 15 kV, 1 and 10 minutes).

Time duration		1 min		10 mins	
Airflow rate		2 m/s	5 m/s	2 m/s	5 m/s
Solution Color		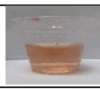	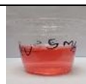	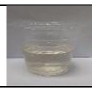	
HEX		925F42	C0372D	847D75	99886E
RGB	RED	146	192	132	153
	GREEN	95	55	125	136
	BLUE	66	45	117	110
CIE Lab*	L	45.20	44.42	52.79	57.57
	a	17.51	53.75	1.17	2.22
	b	25.04	37.86	5.30	16.32

This behavior reflects the coupling between plasma chemistry and mass-transfer dynamics, highlighting the importance of optimizing airflow conditions rather than maximizing gas throughput alone.

3.4 Effect of chamber count: staged plasma enhancement

The chamber count represents the number of axially aligned coaxial discharge units arranged along the airflow direction (Figure 7). Table 4 summarizes the influence of one-, two-, and three-chamber configurations at 15 kV.

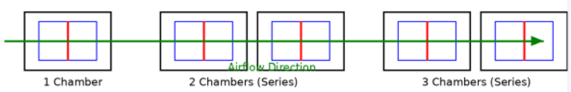

Fig. 7. Illustration of electrodes chamber arrangement.

Table 4. Influence of electrodes chamber count on ozonation performance (15 kV, 1-10 minutes).

Airflow rate	Chamber count	Initial a*	Final a*	Effectiveness
5 m/s	1	53.75	2.22	Moderate
	2	49.20	1.83	High
	3	34.37	0.66	High
2 m/s	1	17.51	1.17	High

	2	14.40	-0.01	Very high
	3	4.73	-0.01	Very high

Increasing the number of chambers significantly enhances decolorization effectiveness. For example, at 2 m/s, the three-chamber configuration achieves near-complete chromatic neutrality ($a^* \approx 0$). This improvement can be attributed to cumulative plasma exposure: as the airflow passes sequentially through multiple discharge zones, ionization events and ozone generation occur in a staged manner.

Importantly, this enhancement does not require increasing the local electric-field intensity, thereby preserving dielectric integrity. The staged architecture therefore provides a scalable geometric strategy for ozone intensification, distinguishing it from approaches that rely solely on higher voltage.

3.5 Electrical power consumption and energy trade-off

Leakage-current measurements were conducted to evaluate discharge-related electrical losses. As shown in Table 5 and Figure 8, both applied voltage and chamber count increase the measured apparent power.

Table 5. Power loss as a function of leakage current and applied voltage.

Chamber count	Voltage (kV)	Leakage Current (μA)	Power Loss (W)
1	5.47	195.03	1.07
	10.37	691.30	7.17
	15.46	1058.00	16.35
2	5.36	431.03	2.31
	10.34	1195.30	12.35
	15.26	1837.00	28.03
3	5.23	587.30	3.07
	10.32	1627.60	16.79
	15.46	2609.30	40.33

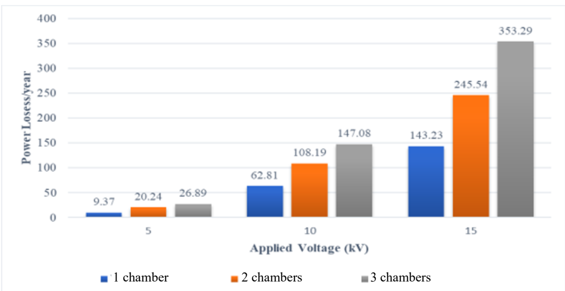

Fig. 8. Relationship between the power losses and the applied voltage as well as the electrodes chamber count.

While multi-chamber configurations improve ozonation performance, they also increase electrical consumption due to cumulative capacitive effects and the larger effective discharge volume.

All measurements were repeated three times under identical conditions, with observed variations below 5%, confirming acceptable experimental repeatability.

It should be noted that the power values represent apparent discharge power ($P = U \cdot I$). Since phase-angle measurements were not performed, true discharge power may differ slightly. However, because identical measurement procedures were applied across all configurations, comparative performance trends remain valid.

3.6 Energy-normalized decolorization efficiency

To further evaluate the energy–performance trade-off, decolorization effectiveness was normalized with respect to discharge power. Figure 9 presents the normalized decolorization efficiency ($\Delta a^*/W$) as a function of chamber count at 15 kV and 2 m/s.

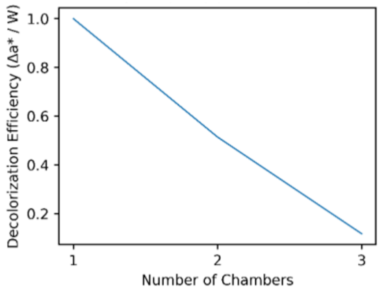

Fig. 9. Decolorization efficiency normalized by discharge power ($\Delta a^*/W$) as a function of chamber count at 15 kV and 2 m/s.

Although total decolorization improves with increasing chamber count, the normalized efficiency per unit power decreases slightly. This indicates that the incremental gain in chromatic removal becomes smaller relative to the additional electrical energy supplied. Therefore, chamber optimization should consider both absolute performance and energy-normalized effectiveness.

The influence of airflow rate on energy-normalized efficiency is further illustrated in Figure 10. Operation at 2 m/s consistently exhibits higher $\Delta a^*/W$ values compared to 5 m/s across all chamber configurations. The difference becomes more pronounced at higher chamber counts. For example, at the three-chamber configuration, the normalized efficiency at 2 m/s is notably higher than at 5 m/s, emphasizing the importance of residence-time control in maximizing ozone utilization.

These results demonstrate that airflow rate is a critical parameter not only for absolute ozonation performance but also for energy-normalized efficiency, reinforcing the need for integrated optimization of electrical and fluid-dynamic parameters in multi-chamber DBD reactor design.

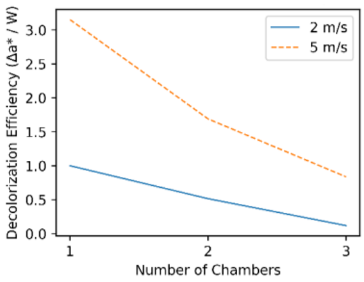

Fig. 10. Comparison of decolorization efficiency normalized by discharge power (Δa*/W) for airflow velocities of 2 m/s and 5 m/s at 15 kV and 10 minutes of treatment.

3.7 Estimated ozone production yield

Although direct ozone concentration measurements were not conducted, an approximate ozone production rate can be estimated from the measured electrical power combined with ozone yield ranges reported in the literature [2], [5].

For the three-chamber configuration operating at 15 kV with an electrical input of 40.33 W, the estimated ozone production rate ranges from approximately 0.8 to 4.8 g/h based on typical ozone energy-yield values reported in the literature. While this estimation does not replace standardized concentration measurement techniques such as UV absorption or iodometric titration, it provides a quantitative reference for comparing the proposed reactor with previously reported DBD ozone generators.

Future work will incorporate direct ozone concentration measurements using standardized analytical techniques. Dissolved ozone in aqueous systems is commonly quantified using the indigo trisulfonate colorimetric method, which enables stoichiometric spectrophotometric determination of ozone concentration [9]. In addition, gas-phase ozone concentration may be evaluated using UV absorption at 253.7 nm to obtain standardized ozone yield metrics (g/kWh). These estimated values fall within the typical range reported for atmospheric-pressure DBD ozone generators, indicating that the proposed multi-chamber configuration achieves competitive ozone production performance.

3.8 Limitations of power characterization

It is acknowledged that accurate power characterization in DBD systems ideally requires Q–V Lissajous methods or simultaneous voltage–current waveform analysis to determine true discharge power. In the present work, phase-angle information was not measured; therefore, the reported values represent apparent discharge power. However, since identical measurement procedures were consistently applied to all reactor configurations, the comparative trends regarding chamber count, applied voltage, and airflow rate remain valid for design-performance evaluation.

4 Conclusions

This study demonstrates that a multi-chamber coaxial Dielectric Barrier Discharge (DBD) reactor can effectively enhance ozone generation through staged axial plasma exposure while maintaining dielectric integrity. Finite-element simulations confirmed strong electric-field localization within the 1-mm annular air gap, supporting intensified ionization without excessive dielectric stress.

Experimental results show that applied voltage is the dominant factor governing ozone formation, with 15 kV producing the most significant chromatic degradation. Airflow velocity strongly influences ozone utilization, where operation at 2 m/s improves residence time and plasma stability compared to 5 m/s. Increasing the chamber count from one to three chambers enables cumulative plasma exposure and achieves near-complete decolorization under optimal conditions.

Electrical measurements reveal increasing apparent power consumption with additional chambers, highlighting a fundamental trade-off between ozonation performance and energy input. Energy-normalized analysis indicates that while total decolorization increases with chamber count, efficiency per unit power slightly decreases. The estimated ozone production rate for the three-chamber configuration at 15 kV ranges from 0.8 to 4.8 g/h.

Overall, the proposed staged multi-chamber architecture provides a scalable and energy-conscious strategy for improving ozone generation in environmentally compatible water-treatment systems.

Declaration on the use of AI and AI-assisted tools: AI-assisted tools were used only for language editing and improving clarity. All scientific content, analyses, figures, and conclusions were developed and verified by the authors, who take full responsibility for the manuscript.

References

1. M. Amirbande and A. Vahedi, Mathematical modeling of the electric field in planar and coaxial dielectric barrier discharge reactors for water treatment. Compel. **41**, 5, 1398–1414 (2022). https://doi.org/10.1108/COMPEL-08-2021-0309
2. D. Korzec, F. Freund, C. Bäuml, P. Penzkofer, and S. Nettesheim, Hybrid dielectric barrier discharge reactor: Characterization for ozone production. Plasma. **7**, 3, 585-615 (2024). https://doi.org/10.3390/plasma7030031
3. F. Liu, Y. Wang, W. Wang, G. Shi, Z. Fan, J. Wang, and H. Han, Generation of the high power by a coaxial dielectric barrier discharge with a perforated electrode in atmospheric pressure air. Phys. of Plasm. **30**, 9 (2023). https://doi.org/10.1063/5.0160137
4. V. Luvita, AT Sugiarto, and S. Bismo, Characterization of dielectric barrier discharge reactor with nanobubble application for industrial water treatment and depollution. SAJCE. **40**, 1,

246-257 (2022). https://doi.org/10.1016/j.sajce.2022.03.009

5. L. Xie, D. Yuan, C. Jin, H. Xu, Y. Li, L. Wei, W. Wu, and Z. Ling, Characteristics of dielectric barrier discharge and ozone production in synthetic air. Vacuum. **226**, 113359 (2024). https://doi.org/10.1016/j.vacuum.2024.113359
6. M. Mahmoodi and E. Pishbin, Ozone-based advanced oxidation processes in water treatment: Recent advances, challenges, and perspective. Environ. Sci. Pollut. Res. **32**, 7, 3531-3570 (2025). https://doi.org/10.1007/s11356-024-35835-w
7. U. Kogelschatz, Dielectric-barrier discharges: Their history, discharge physics, and industrial applications. Plasm. Chem. and Plasm. Proc. **23**, 1, 1–46 (2003). https://doi.org/10.1023/A:1022470901385
8. R. Brandenburg, Dielectric barrier discharges: progress on plasma sources and on the understanding of regimes and single filaments. Plasma Sources Sci. Technol. **26**, 053001, 1-29 (2017). https://doi.org/10.1088/1361-6595/aa6426
9. H. Bader and J. Hoigné, Determination of ozone in water by the indigo method. Water Res. **15**, 4, 449–456 (1981). https://doi.org/10.1016/0043-1354(81)90054-3